Available online at www.sciencedirect.com
SCIENCE DIRECT
Polymer 47 (2006) 5097–5107
polymer
www.elsevier.com/locate/polymer

Structural studies of electrospun cellulose nanofibers

Choo-Won Kim [a], Dae-Sik Kim [a], Seung-Yeon Kang [a], Manuel Marquez [b,c], Yong Lak Joo [a,*]

[a] *School of Chemical and Biomolecular Engineering, Cornell University, Ithaca, NY 14853, USA*
[b] *Phillip Morris USA, 4201 Commerce Road, Richmond, VA 23234, USA*
[c] *Chemical Sciences and Technology Division, Los Alamos National Laboratory, Los Alamos, NM 87545, USA*

Received 3 March 2006; received in revised form 11 May 2006; accepted 14 May 2006
Available online 5 June 2006

Abstract

Non-woven mats of submicron-sized cellulose fibers (250–750 nm in diameter) have been obtained by electrospinning of cellulose solutions. Cellulose are directly dissolved in two solvent systems: (a) lithium chloride (LiCl)/*N*,*N*-dimethyl acetamide (DMAc) and (b) *N*-methylmorpholine oxide (NMMO)/water, and the effects of (i) solvent system, (ii) the degree of polymerization of cellulose, (iii) spinning conditions, and (iv) post-spinning treatment such as coagulation with water on the miscrostructure of electrospun fibers are investigated. The scanning electron microscope (SEM) images of electrospun cellulose fibers show that applying coagulation with water right after the collection of fibers is necessary to obtain submicron scale, dry and stable cellulose fibers for both solvent systems. X-ray diffraction studies reveal that cellulose fibers obtained from LiCl/DMAc are mostly amorphous, whereas the degree of crystallinity of cellulose fibers from NMMO/water can be controlled by various process conditions including spinning temperature, flow rate, and distance between the nozzle and collector. Finally, electrospun cellulose fibers are oxidized by HNO_3/H_3PO_4 and $NaNO_2$, and the degradation characteristics of oxidized cellulose fibers under physiological conditions are presented.

Keywords: Cellulose; Electrospinning; Oxidation

1. Introduction

Cellulose is a naturally occurring polymer of particular interest due to its abundant availability and biodegradability. These properties make cellulose fibers useful in a wide range of areas, such as filtration, biomedical applications, and protective clothing [1]. Nonetheless, processing of cellulose is restricted by its limited solubility in common solvents and its inability to melt because of its numerous intermolecular and intra-molecular hydrogen bonding [1]. Earlier cellulose fibers were produced via wet spinning and involved derivatization of the polymer. In wet spinning, cellulose mixed with binders is fed to the spinneret, which is submerged in a chemical bath, and the fibers are collected as the solution emerges and the polymer filaments are precipitated and solidified [1,2]. In the viscose process, cellulose derivatized into its xanthate form and sulfuric acid/zinc has been used as a coagulant to regenerate cellulose fibers [1]. However, this process includes several side reactions and extra purification steps. Alternatively, cellulose fibers have been obtained from its derivatives such as cellulose acetate by converting their fibers into cellulose [3]. The conversion into cellulose is incomplete and final fibers contain a mixture of cellulose and cellulose acetate. Recently, cellulose was directly spun from *N*-methylmorpholine oxide (NMMO)/water commercially [2]. These fibers are commonly known as Lyocell fibers and are obtained via dry-jet wet spinning. Lyocell fibers tend to have high modulus and orientation but low elongation [1].

Electrostatic fiber spinning or 'electrospinning' is a novel process for forming fibers with submicron scale diameters through the action of electrostatic forces. When the electrical force at the interface of a polymer liquid overcomes the surface tension, a charged jet is ejected [4]. The jet initially extends in a straight line then undergoes a vigorous whipping motion caused by the electrohydrodynamic instability [5,6]. As the solvent evaporates, the polymer is collected onto a grounded mesh or plate in the form of a non-woven mat with high surface area to mass ratio (10–1000 m^2/g). These non-woven mats are finding uses in filtration, protective clothing and biomedical applications [7–10]. The development of value-added products with large surface area from abundant cellulose in nature via electrospinning could significantly expand its applications and

* Corresponding author. Tel.: +1 607 255 8591; fax: +1 607 255 9166.
E-mail address: ylj2@cornell.edu (Y.L. Joo).

0032-3861/$ - see front matter © 2006 Elsevier Ltd. All rights reserved.
doi:10.1016/j.polymer.2006.05.033

usages. Although electrospinning has recently been applied to obtain cellulose fibers [11–13], a thorough study on the structure–electrospinning–solvent relationship has not been done.

The objective of the current study is to investigate the effect of (i) solvent system (ii) degree of polymerization (DP), (iii) processing conditions and (iv) post-spinning treatment on the microstructure of submicron-scale, electrospun cellulose fibers. In particular, we are interested in how the degree of crystallinity of electrospun fibers is influenced by these parameters. We chose two well-studied solvent systems for cellulose: lithium chloride (LiCl)/*N*,*N*-dimethyl acetamide (DMAc) and *N*-methylmorpholine oxide (NMMO)/water. The LiCl/DMAc solvent system has shown to dissolve cellulose from different sources for a large range of cellulose concentrations without side reactions [14,15], but solution preparation involves lengthy and complex swelling and conditioning steps. The presence of lithium chloride, not any other salts, has shown to be necessary to bridge the electrostatic interaction between DMAc and cellulose [16,17]. On the other hand, the range of NMMO/water composition suitable for spinning cellulose is very narrow [18,19] and elevated temperature is necessary for spinning. However, the solution preparation for the NMMO/water system is much simpler than that for LiCl/DMAc.

In addition, since it has demonstrated that the NMMO and water solvent mixture can effectively be recovered as in the commercial Lyocell process (more than 99.9% recovery) [20], it is environmentally friendly and may provide a closed-loop solvent electrospinning process. Unlike in LiCl/DMAc, cellulose does not form ionic complexes with NMMO and water during its dissolution. The presence of water allows NMMO to penetrate cellulose macromolecules [21], and NMR studies have shown that NMMO undergoes conformational modification in the presence of cellulose [22]. Dissolution of cellulose is limited by the amount of water in the tertiary system, or namely water to NMMO molar ratio (n). In fact, only NMMO hydrates with n of about 1 or lower can completely dissolve cellulose [18,21,22].

In the present paper, we will summarize the effect of DP, processing, and post treatment on the morphology of electrospun cellulose fibers from two different solvents. Our results reveal that applying coagulation with water right after the collection of fibers is necessary to obtain submicron scale, dry and stable cellulose fibers for both solution systems. We then will demonstrate that cellulose fibers obtained from LiCl/DMAc are mostly amorphous, whereas the degree of crystallinity of cellulose fibers from NMMO/water can be controlled by various process conditions including spinning temperature, flow rate, and distance between the nozzle and collector. Finally, electrospun cellulose fibers are oxidized with HNO_3/H_3PO_4 and $NaNO_2$. Oxidized cellulose (OC) is a material highly desirable in biomedical applications due to its nontoxicity and fast degradability under physiological conditions [23]. However, due to its poor solubility in common solvents, production of oxidized cellulose fibers has been achieved by spinning cellulose or cellulose derivatives followed by the oxidization of obtained fibers. Since, we can easily surmise that the biocompatibility and degradability of oxidized cellulose fibers would depend on its morphology and the degree of oxidation, we would like to utilize electrospun cellulose fibers to develop highly oxidized cellulose with large surface area. The degradation characteristics of oxidized cellulose fibers under physiological conditions are presented.

2. Experiments

2.1. Materials

All chemicals used in the study are of analytical grade and were obtained from commercial sources. DMAc (Sigma–Aldrich) and high performance liquid chromatography water (Mallinckrodt) were used without further purification. Lithium chloride was obtained from Merck. Ninety–seven percent NMMO powder, 50% aqueous NMMO solution, and *n*-propyl gallate were obtained from Sigma–Aldrich. Cellulose with two different degrees of polymerization (DP), fibrous cellulose CF-11 powder (DP of 210) and surgical cotton batting (DP of 1140) was used in the study. Cellulose materials were ground to 20 mesh in a Wiley mill. High performance liquid chromatography water, acetone, KH_2PO_4, K_2HPO_4, $NaNO_2$, H_3PO_4 (85.8%), and HNO_3 (69.7%) from Mallinckrodt Chemicals, and 200 proof ethanol from Pharmco Products were employed without further purification in the oxidation study.

2.2. Solution preparation

For the LiCl/DMAc system, cellulose powders of DP 1140 were pretreated with water for a period of at least 8 h at room temperature ($\sim$20 °C). After the sample was dried under vacuum at 60 °C, cellulose solutions were prepared by dissolving fine cellulose particles in LiCl/DMAc with constant stirring at 50–60 °C for 2 h. The cellulose solutions were further mixed for 12 h at room temperature. The conditioning of cellulose was found to be critical for complete dissolution. Dried cellulose was conditioned in water prior to solvent exchange, and heated at 60 °C. Heating was necessary for the complete dissolution of polymer. However, the temperature of the solution was kept below 80 °C to avoid degradation. The concentration of DP1140 cellulose in LiCl (8 wt%)/DMAc from 1 to 3 wt% was used in the current study.

For the NMMO/water system, cellulose was placed in vacuum oven at 80 °C for about 8 h before it was used for solution preparation. An appropriate amount of 97% NMMO powder, cellulose, and propyl gallate was placed in a vial and mixed vigorously at room temperature. The mass of antioxidant (propyl gallate) was 0.5–1% of that of cellulose. 50% NMMO/water was added slowly to achieve the desired solution composition. The weight ratio of NMMO to water in the final solution was about 85/15% (w/w), which is equivalent to a molar ratio of 1/1 ($n=1$). Samples were heated at 120 °C for 1 h or until the complete dissolution of cellulose, and they were manually stirred every 10–15 min. One to three weight

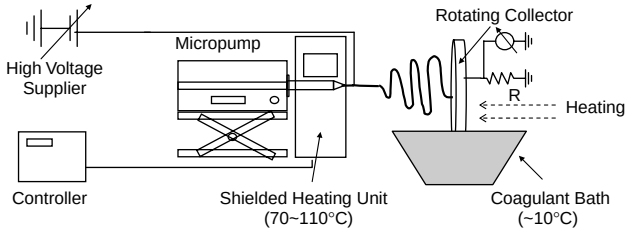

Fig. 1. Schematic diagram of the electrospinning system used in the current study.

percent of DP1140 cellulose or 9 wt% of DP210 cellulose in NMMO/water was used in the current study.

2.3. Electrospinning

The schematic of electrospinning setup used in this study is depicted in Fig. 1, and Table 1 summarizes the differences in conditions between two solvent systems.

Homogeneous cellulose solution was loaded in the syringe and placed in the micropump. For the LiCl/DMAc system, electrospinning was carried out at room temperature, while the temperature of the syringe and the needle was controlled to remain at 70–110 °C during the spinning process from NMMO/water. A flat aluminum plate or mesh was placed 10–20 cm away from the tip of the nozzle to collect fibers under various operating conditions. Electrospinning of cellulose solutions was conducted over a wide range of electric field strengths (1–4 kV/cm) by varying the voltage drop for a preset distance and using a number of different flow rates, usually less than 0.05 ml/min. The heating was applied to the collector, followed by coagulation with water for the LiCl/DMAc system to effectively remove DMAc and LiCl, while the temperature of the collector was kept below the room temperature (9–10 °C) for the NMMO/water system to promote fast solidification of fibers. Note that the coagulation process was applied right after dry fibers were collected on the rotating collector for both solvent systems. Samples were subject to coagulation in water before being completely dried under vacuum at 60 °C.

2.4. Characterizations

The molecular weight of the samples was measured via the intrinsic viscosity measurement according to ASTM D4243 using a capillary viscometer. Degradation was also monitored during the study by measuring the intrinsic viscosity and thus the molecular weight of the final products. The morphology of collected fibers was analyzed using scanning electron microscope (SEM). The rheological properties of cellulose solution were obtained from Dynamic Analyzer RDA II. Wide angle X-ray scattering (WAXS) was employed to determine the crystalline structures of cellulose fibers. The degree of crystallinity was obtained by the area ratio of the crystalline phase to the total phases (crystalline and amorphous phases) after deconvoluting each peak in the WAXS pattern.

Table 1
Comparison of electrospinning conditions for two solvent systems

Solvent system	Solution temperature	Collector temperature	Coagulation temperature
DMAc/LiCl	Room temperature (RT)	Heated (~100 °C)	RT
NMMO/water	Heated (70–110 °C)	<RT	Cooled (9–10 °C)

2.5. Oxidation of cellulose fibers

DP1140 cellulose fibers obtained from LiCl/DMAc were dried under vacuum for 2 h prior to oxidation. Dried samples were then placed in a vial containing HNO3/H3PO4 (2:1 v/v) [23]. The ratio of cellulose mass to acidic mixture was 1 g/14 ml. Once the cellulose fiber mat was completely soaked, 0.2 g of $NaNO_3$ for every gram of cellulose fiber was added at once. The reaction was left to proceed in an enclosed vial for 12, 24, or 48 h. Occasionally, mechanical stirring was applied to the samples for homogeneous reaction. Oxidation was stopped by washing samples with water until the filtrate pH was above 4. Finally, the samples were washed with acetone, and left to dry under ambient conditions. The degree of oxidation was determined by the presence of carboxyl groups in the Fourier transform infrared (FT-IR) spectra.

2.6. In vitro degradation experiments

The initial mass of 4 vacuum dried 6-carboxylcellulose mats was weighted. They were then placed in a buffer solution (KH_2PO_4/K_2HPO_4) of pH 7 at 37 °C. The degradation of each sample was terminated at various reaction times (1, 2, 3, and 5 days) by washing the samples with water during vacuum filtering. The mass of recovered oxidized cellulose in each case was measured after vacuum drying, and the mass loss over time was recorded.

3. Results and discussion

3.1. Solution rheology

Cellulose with two different molecular weights (DP = 210 and 1140) was used in the study. To determine spinning temperature for the NMMO/water system, a solution containing 9 wt% DP210 cellulose in NMMO/water, and solutions with two different concentrations 1.5 and 2 wt% of DP1140 in NMMO/water were prepared, and the shear rheology of these cellulose solutions was obtained in parallel plates at various temperatures and is shown in Fig. 2. The viscosity of 3 wt% DP1140 in LiCl/DMAc at room temperature is shown for comparison. It is observed that the shear viscosity of cellulose solutions is sensitive to solution temperature and the activation energy is comparable to that of polymer melt systems ($E_a/R = 2900$ K for 9 wt% of DP210 cellulose, where E_a is the activation energy and R is

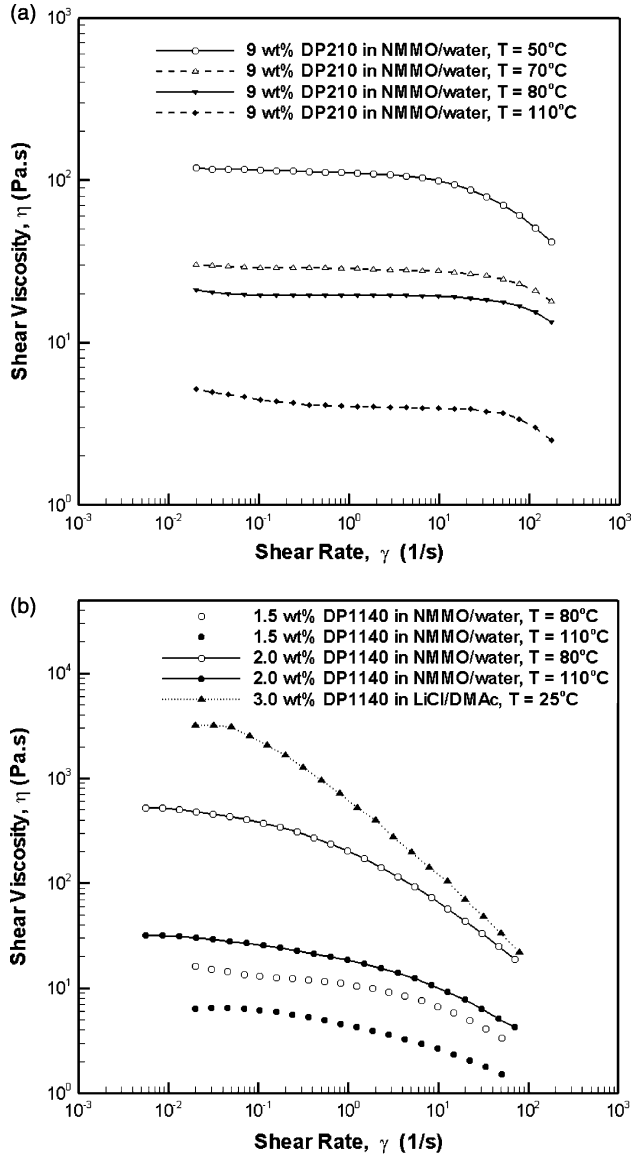

Fig. 2. Shear viscosity of cellulose/NMMO/water solution at various temperatures: (a) 9.0 wt% DP210 cellulose, and (b) 1.5 and 2.0 wt% DP1140 cellulose. The viscosity of 3 wt% DP1140 cellulose in LiCl/DMAc at room temperature is also shown for comparison.

the gas constant). We also note that the shear viscosity of solutions with high molecular weight cellulose strongly depends on shear rate. For example, a solution with 1.5 wt% DP1140 cellulose exhibits a significant shear thinning behavior than that with 9 wt% DP210 cellulose at 80 °C, while the zero shear rate viscosity of two solutions is comparable at 80 °C. The degree of shear thinning for solutions with DP1140 cellulose increases with increasing its concentration. A higher degree of shear thinning has also been observed in the previous rheology studies of high molecular weight cellulose in NMMO/water systems [19,24]. It is also seen that the viscosity of 3 wt% DP1140 cellulose in LiCl/DMAc at high shear at room temperature is only slightly higher than that of 2 wt% DP1140 in NMMO/water at 80 °C due to significant shear thinning. Despite its high viscosity, the cellulose solution was successfully electrospun because of its high charge density from the polar polymer and solvent, and its shear thinning nature at relatively high voltage and flow rate.

3.2. Effect of processing conditions and degree of polymerization on fiber morphology

The operating conditions for the continuous production of cellulose fibers were thoroughly investigated. The optimum range of voltage was between 15 and 25 kV at the distance between the nozzle and the collector, d, of 10–20 cm. The flow rate, Q, ranged from 0.005 to 0.03 ml/min. Fibers were collected on an aluminum plate or mesh, and the morphology of fibers was then examined using SEM. When fibers were collected on a stationary collector at room temperature without coagulation, they were still wet even at a very low flow rate ($Q=0.005$ ml/min) and merged forming a film-like structure as shown in the SEM images from both solvent systems (Fig. 3).

Thus, in order to obtain dry fibers, LiCl/DMAc or NMMO/water had to be removed more efficiently as fibers came in contact with the collector or it must have come in contact with water for coagulation. First, commercial filter media for dust collection that has three-dimensional morphology of thick cellulose fibers was utilized as a collector

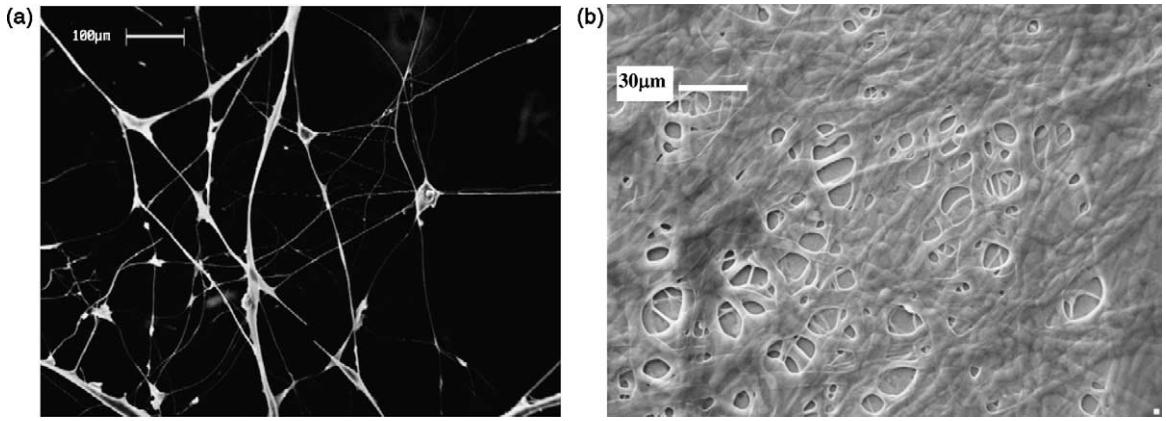

Fig. 3. SEM images of electrospun fibers/film without coagulation (a) from 3 wt% DP1140 cellulose/LiCl/DMAc at room temperature, and (b) from 9 wt% DP210 cellulose/NMMO/water solution collected on a stationary aluminum mesh at $T_{nozzle}=70$ °C. For both cases, $Q=0.005$ ml/min, and $d=15$ cm.

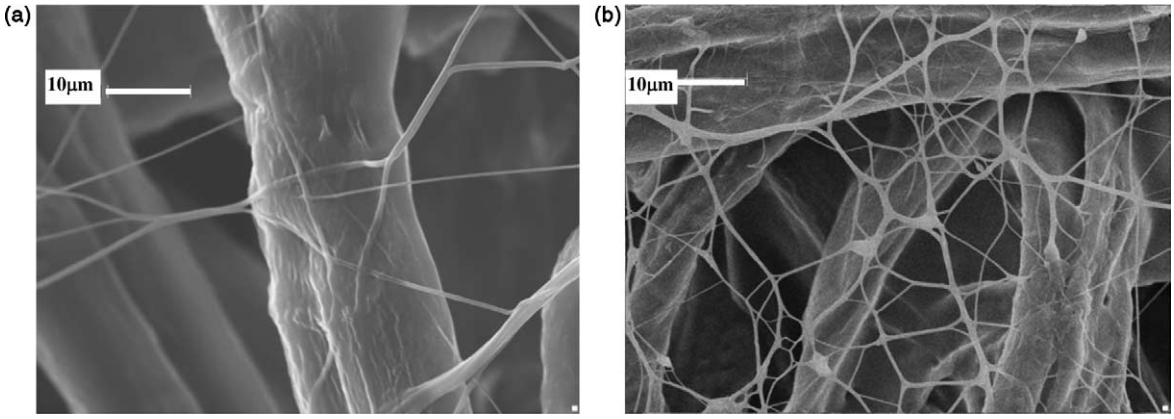

Fig. 4. SEM image of electrospun fibers on filter media (a) from 3 wt% DP1140 cellulose/LiCl/DMAc at room temperature, and (b) from 9wt% DP210 cellulose in NMMO/water on cellulose filter media without coagulation at $T_{nozzle}=50$ °C. $Q=0.01$ ml/min, and $d=15$ cm.

and 3 wt% DP1140 in LiCl/DMAc and 9 wt% DP210 in NMMO/water were electrospun onto cellulose filter media without coagulation. The SEM image of cellulose nanofibers on cellulose filter media is shown in Fig. 4.

Unlike fibers collected on the aluminum plate or mesh, those on the filter media remained uniform and dried without the coagulation process for both solvent systems. The three dimensional morphology of thick and coarse cellulose filter seemed to aid more effective removal of DMAc or NMMO/-water from electrospun fibers after they were collected. In addition, non-woven cellulose filter were partly solvated by the residual solvent in electrospun fibers. As a result, a good adhesion between the electrospun cellulose fibers and the cellulose filter media is observed. In fact, some of the electrospun fibers are partially merged to the larger cellulose fiber filter. Electrospinning cellulose nanofibers on cellulose filter media could lead to simpler production of higher performance filters as well as easy recycling of the products.

Secondly, a rotating collector that partially immerses into cold water for coagulation was incorporated into the electrospinning process as depicted in Fig. 1. The resulting fiber morphology varied depending on the rotation speed of the collecting disk, as shown in Fig. 5.

At 1.2 rpm, the collector had enough time emerging from a water bath to be nearly dry with a very thin layer of water for the deposition of additional fibers. This allowed the collection of uniform and stable fibers. On the other hand, as the rotation speed of the collector was increased, the rotating collector became wetter and a much thick layer of water was noticeable. This confirms the result of electrospinning experiments with cellulose/NMMO/water solutions by Kang et al. [11] where coagulation with water was applied before collecting fibers on a collector. Their fibers were in general larger (3–10 μm) and non-uniform. Thus, the rotating velocity of the collector is a critical parameter for the collection of uniform electrospun fibers.

Hence, all the following experiments were conducted using a rotating collector with a water coagulation bath. In case of the NMMO/water system, the morphology of electrospun fibers was significantly influenced by processing conditions such as nozzle temperature and flow rate. SEM images of DP210 cellulose fibers that were electrospun at three different nozzle temperatures are shown in Fig. 6. It is observed that fibers obtained at three different nozzle temperatures are uniform in size and their average diameter is below 1 μm. In particular, the average diameter of DP210 cellulose fibers electrospun at

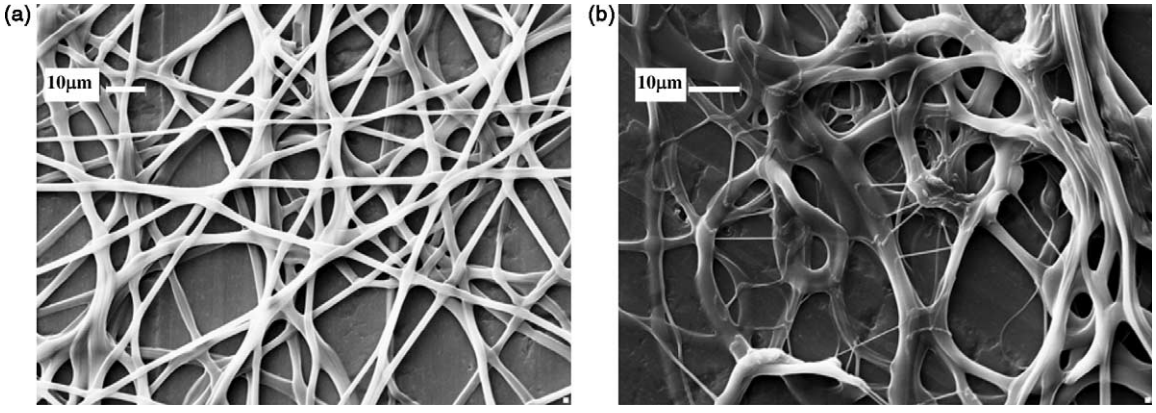

Fig. 5. SEM images of electrospun fibers from 9 wt% DP210 cellulose/NMMO/water solution with a rotating collector at: (a) 1.2 rpm, and (b) 6 rpm. Flowrate was kept at 0.03 ml/min.

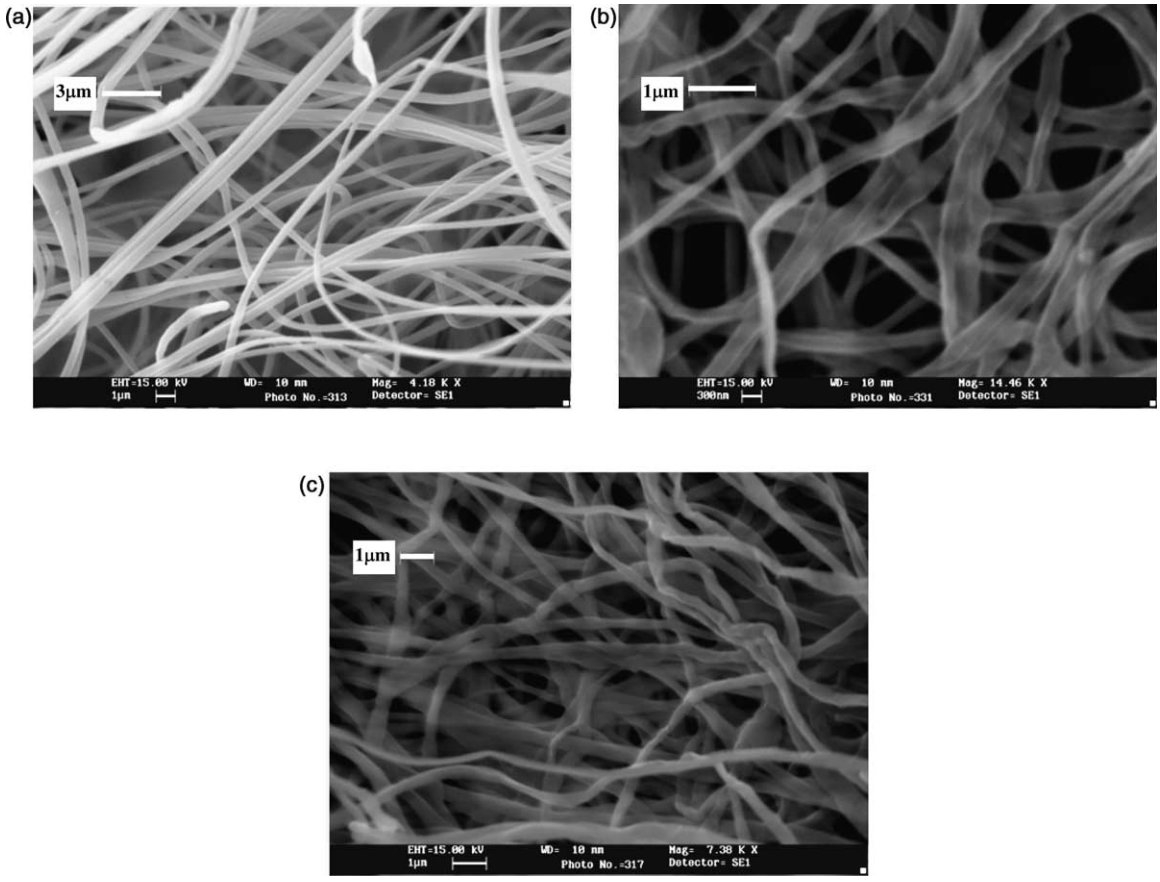

Fig. 6. SEM images of electrospun fibers from 9 wt% cellulose/NMMO/water solution with flow rate 0.01 ml/min and distance 15 cm: (a) $T_{nozzle}=50$ °C, (b) $T_{nozzle}=70$ °C, and (c) $T_{nozzle}=90$ °C.

70 °C is about 300 nm (Fig. 6(b)). Spinning the same cellulose solution at different nozzle temperatures (50 and 90 °C) under the same processing conditions produced thicker fibers (750 and 450 nm, respectively). A nozzle temperature above 90 °C or flow rate below 0.01 ml/min lead to a frequent breakage of the jet, possibly due to a decrease in the extensional viscosity [25,26]. Producing continuous thin fibers at nozzle temperature below 50 °C was not achieved due to the high viscosity of the solution.

Three different compositions (1.5, 2 and 2.5 wt%) of DP1140 cellulose in NMMO/water were electrospun at two different nozzle temperatures ($T_{nozzle}=50$ and 70 °C) and the morphology of successfully electrospun DP1140 cellulose fibers is shown in Fig. 7. Again, submicron scale fibers were obtained for all the cases. We note that the average fiber diameter of DP1140 cellulose fibers (250–750 nm) is in general comparable to those of DP210 cellulose fibers, but the increase in the amount of solvent in higher DP cellulose solutions made it harder to obtain dry fibers. It is observed that fibers become wet and tend to form a film, as the cellulose concentration decreases. This becomes more noticeable when the nozzle temperature was low ($T_{nozzle}=$ 50 °C) and thus the removal of the solvent (NMMO and water) was less efficient. As a result, a high concentration of DP1140 cellulose (2.5 wt%) was needed to obtain dry fibers at nozzle temperature of 50 °C, while 1.5 wt% DP1140 cellulose solution still produced dry fibers at higher nozzle temperature, $T_{nozzle}=70$ °C.

For the LiCl/DMAc system, heating the collector greatly enhances the stability of the fiber morphology, but the removal of both DMAc by heating the collector and salt by coagulation was necessary for the fabrication of dry and stable cellulose fibers. As seen in Fig. 8, a low concentration of cellulose (1 wt% DP1140 in LiCl/DMAc) lead to irregular-shaped clusters of varying sizes (10–100 μm) on the submicron scale fiber mat, whereas fibers from 3 wt% DP1140 cellulose solution does not display such clusters. This indicates a higher concentration is desirable for the timely and complete removal of solvent and salt. Again, there was a slight increase in fiber diameter with increasing cellulose concentration due to the lower extent of solvent evaporation.

The degree of polymerization of cellulose before and after electrospinning was determined from the intrinsic viscosity measurement and summarized in Table 2. Although, the DP of cellulose shows little or no degradation (less than 4% decrease in the molecular weight) of cellulose during electrospinning from LiCl/DMAc, cellulose nanofibers from NMMO/water solutions at elevated temperature (100 °C) exhibit significant degradation of cellulose. This may be due to the fact that cellulose in NMMO/water was placed in

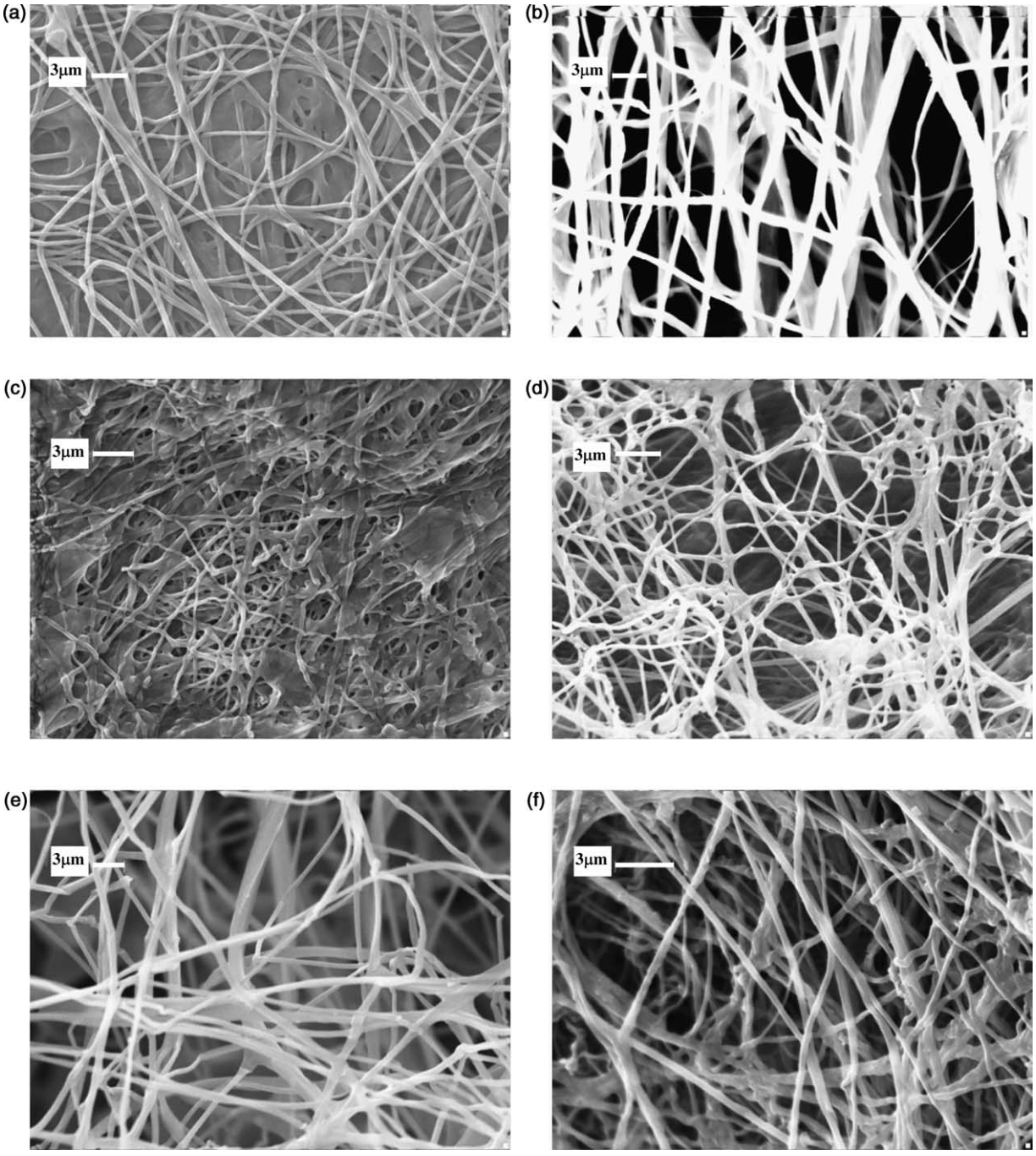

Fig. 7. SEM images of electrospun fibers from DP1140 cellulose in NMMO/water: (a) 1.5 wt%, T_{nozzle} = 50 °C, (b) 1.5 wt%, T_{nozzle} = 70 °C, (c) 2 wt%, T_{nozzle} = 50 °C, (d) 2 wt%, T_{nozzle} = 70 °C, (e) 2.5 wt%, T_{nozzle} = 50 °C, and (f) 2.5 wt%, T_{nozzle} = 70 °C.

a heated chamber at 100 °C for a couple of hours. According to Rosenau et al. side reactions in cellulose in NMMO/water systems at high temperature (both hemolytic (radical) and heterolytic (non-radical) reactions) can lead to degradation of cellulose [27]. On the other hand, the degradation of cellulose fibers from LiCl/DMAc was limited because only the rotating collector was heated where a rapid evaporation of DMAc takes a place at elevated temperature. It should also be noted that the degree of degradation in NMMO/water is more noticeable for cellulose with a higher DP.

3.3. Effect of spinning conditions on crystallization

There was a change in the crystalline structure of cellulose before and after electrospinning. The native cellulose CF-11 powder (DP210) and surgical cotton batting (DP1140) present the crystal form of Type-I, which is the polymorph with the highest degree of intermolecular and intramolecular hydrogen bonding [1]. Electrospun cellulose fibers display a different polymorph. It has been reported that the crystalline polymorph, Type-II forms when cellulose is treated with water or

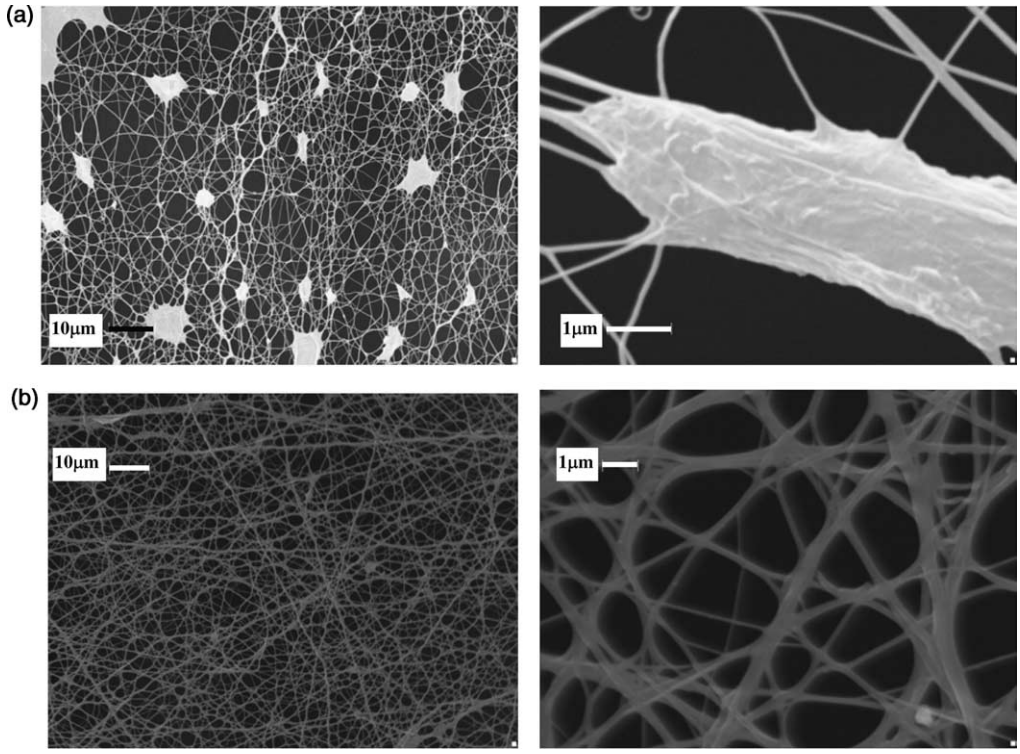

Fig. 8. SEM images of DP1140 cellulose fibers from LiCl/DMAc collected using heated collector followed by coagulation (a) 1 wt% DP1140 and (b) 3 wt% DP1140 in LiCl/DMAc.

methanol, while Type-III forms when cellulose is treated withliquid ammonia [1,28,29]. Since, the dissolution of cellulose in our study involves water, the polymorph expected is Type-II. As shown in Fig. 9, X-ray diffraction studies reveal that electrospun cellulose fibers from LiCl/DMAc are mostly amorphous. This is due to the fact that high temperature was applied at the collector, followed by coagulation with water. Heating the collector can erase any crystal structures developed during spinning and subsequent coagulation with water can act as quenching, which does not favor the re-crystallization of cellulose. We also note that annealing did not help the development of the crystalline phase from amorphous cellulose fibers.

On the other hand, electrospun cellulose fibers from NMMO/water exhibit Type-II cellulose. This is in agreement of structural studies on Lyocell fibers, which also exhibit Type-II cellulose [1,28,29]. We note that DP1140 cellulose from the NMMO/water system was degraded significantly after spinning, and thus DP1140 cellulose fibers from NMMO/water exhibit much lower DP (DP≈600). To determine the degree of crystallinity of electrospun cellulose fibers from NMMO/water, we followed the conventional X-ray analysis, and the deconvolution of the WAXS pattern into two different contributions, amorphous and crystalline phases [28,29]. X-ray diffraction pattern of a typical electrospun DP210 cellulose fiber together with deconvoluted peaks (amorphous at $2\theta = 18.5°$, Type-II crystalline peaks at $2\theta = 12.5$, 20.2 and 22.3°) is shown in Fig. 10(b).

Table 2
Degree of polymerization (DP) of cellulose from intrinsic viscosity measurements

		As received cellulose	Fiber collected at 100 °C	Fiber collected at 25 °C
LiCl/DMAc	DP	1140	1100	1190
		As received cellulose	From solution at 100 °C	Electrospun fibers
NMMO/water	DP	1140	620	580
	DP	210	190	180

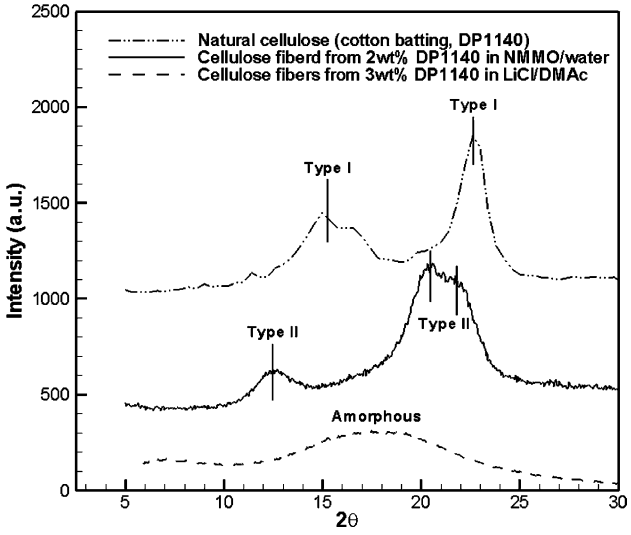

Fig. 9. X-ray diffraction patterns of natural cellulose and electrospun cellulose fibers from two different solution systems (DP=1140).

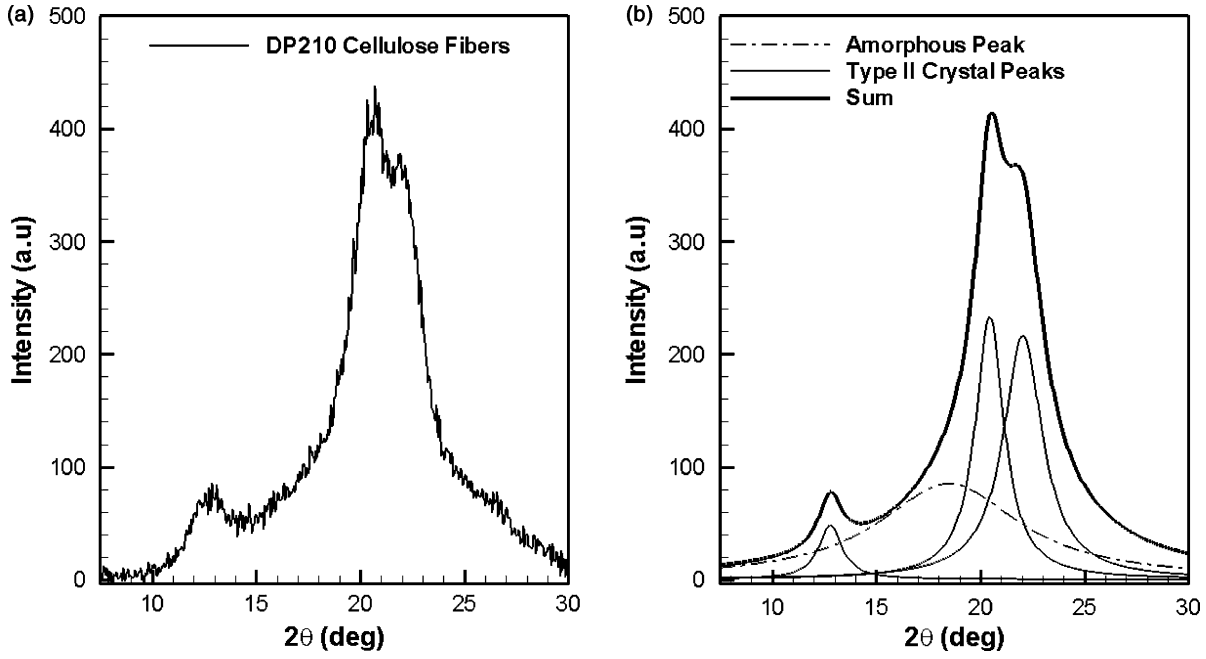

Fig. 10. (a) X-ray diffraction pattern of electrospun cellulose fibers from 9 wt% DP210 in NMMO/water at $T_{nozzle}=70$ °C, $d=15$ cm, and $Q=0.01$ ml/min, and (b) deconvoluted amorphous and Type-II crystalline peaks.

It is observed that the degree of crystallinity of electrospun cellulose fibers from NMMO/water ranges from 40 to 60%. We note that the degree of crystallinity based on the peak heights, i.e. diffraction intensities, I_{002} at 002 peak position and I_{18} at $2\theta=18°$ (amorphous), as a ratio of $[(I_{002}-I_{18})/I_{002}]\times 100$ by Segal [30–32] gives a similar value to that based on the deconvoluted areas of X-ray diffraction patterns (Table 3). The degree of crystallinity of electrospun fibers is also influenced by various process conditions such as flow rate, and distance between the nozzle and collector and they are summarized in Table 3. It is known that the cellulose/NMMO/water solution can crystallize under cooling and the cellulose chains retain the general morphology of the crystallized solution after sublimation of the NMMO and the water [33–35]. Hence, varying the spinning temperature in the NMMO/water system, for example, influences the crystallization of cellulose/NMMO/water solution during electrospinning, and thus the crystallinity of electrospun fibers. It is observed that lower nozzle temperature and thus lower spinning temperature decreases the degree of crystallinity. In addition, a decrease in the degree of crystallinity is observed when the jet had less residence time during electrospinning (i.e. shorter nozzle-to-collector distance and/or higher flow rate) and thus less time for crystallization. Finally, we note that cellulose fibers of higher DP (DP1140) from dilute solution (3 wt%) exhibit a slightly lower degree of crystallinity than those of low DP (DP210) from high concentration (9 wt%) at the same processing condition. Although, cellulose of different origins may not always allow a proper comparison, these results are not in agreement with the isothermal crystallization of cellulose/NMMO/water solutions study by Biganska et al. [34] who reported the crystallization rate does not depend on cellulose DP but the rate decreases strongly with increasing cellulose concentration. This may be due to various complex aspects in electrospinning such as nonisothermal effect, elongational deformation, change in water content via coagulation, etc.

3.4. Oxidation of cellulose and degradation study

DP1140 cellulose fibers electrospun from LiCl/DMAc were subjected to oxidation mediated by $HNO_3/H_3PO_4/NaNO_2$. The

Table 3
Degree of crystallinity of cellulose electrospun fibers at various spinning conditions

Cellulose (%)	Nozzle temperature T_{nozzle} (°C)	Nozzle to collector distance, d (cm)	Flow rate, Q (ml/min)	Degree of crystallinity	
				By peak area	By peak height
DP210 from NMMO/water	50	15	0.01	52.9	58.8
DP210 from NMMO/water	70	15	0.01	56.8	66.5
DP210 from NMMO/water	70	15	0.03	40.4	42.1
DP210 from NMMO/water	70	10	0.01	50.1	45.5
DP1140 from NMMO/water	70	15	0.01	42.2	44.7
DP1140 from LiCl/DMAc	25	15	0.01	~0.0	~0.0

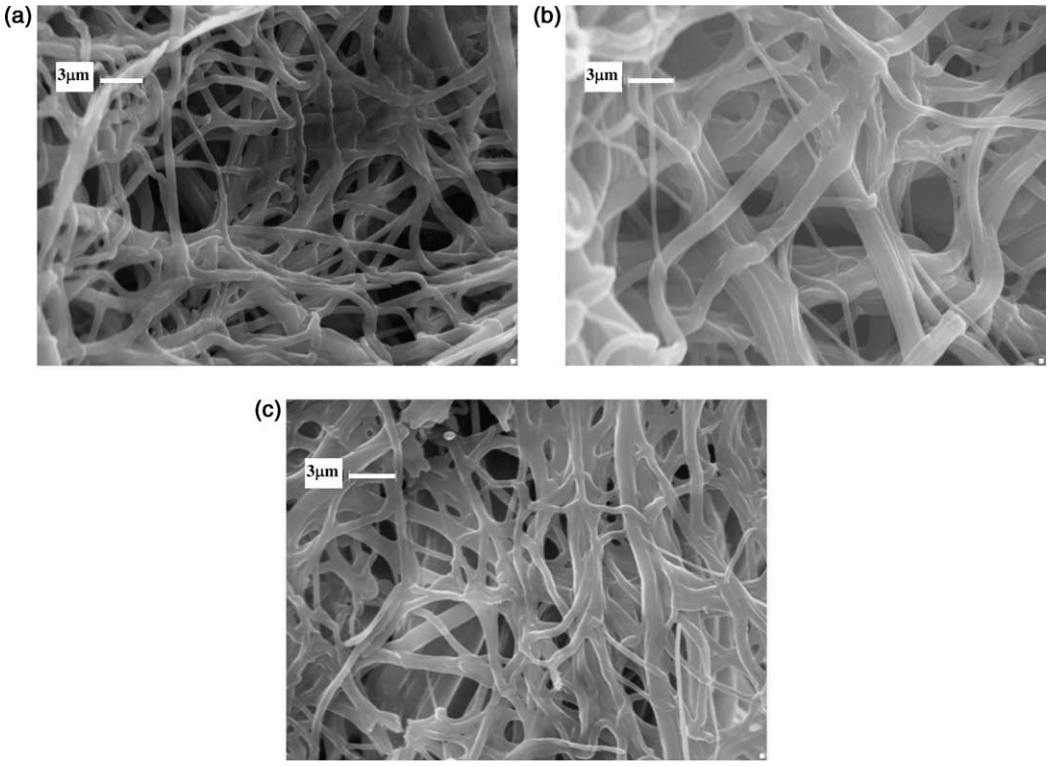

Fig. 11. SEM images of electrospun DP1140 cellulose fibers after oxidation reaction time of: (a) 12 h (b) 24 h, and (c) 48 h.

SEM images of oxidized cellulose fibers at various oxidation times are shown in Fig. 11. It is observed that the overall morphology of oxidized cellulose fibers for various reaction times up to 48 h was comparable to that of as-spun fibers. However, a small degree of deterioration of fiber morphology is apparent on oxidized fibers. From previous work by Kumar et al. it has been known that oxidation is accompanied by undesirable degradation [23]. The extent of degradation becomes more pronounced with increasing oxidation time.

The yield of the oxidative reaction was about 80%, and the presence of carboxyl groups along polymeric chains was detected using FTIR. The characteristic peaks at 1750 cm^{-1} corresponding to C=O group appear in spectrum of oxidized cellulose fibers. The broad peak corresponding to hydroxyl group is observed in both cellulose and oxidized cellulose spectra (Fig. 12).

Fibers after 48 h oxidation degraded rapidly under physiological conditions. The evolution of the mass loss was almost linear in the first 3 days, but the rate of degradation seemed to decrease in the following 48 h yielding a total of 85% mass lost by day 5 (Fig. 13). Since, we can easily surmise that the degradation of oxidized cellulose will depend on the fiber morphology and microstructure, the degradation time can be controlled possibly by changing the average fiber diameter and/or the degree of crystallinity. A more comprehensive study on controlling the degradation of oxidized cellulose and cellulose fibers is underway.

4. Conclusion

We have demonstrated that non-woven mats of submicron-sized cellulose fibers (250–750 nm in diameter) can be obtained by electrospinning cellulose from two different solvent systems: LiCl/DMAc and NMMO/water. The scanning electron microscope (SEM) images of electrospun cellulose

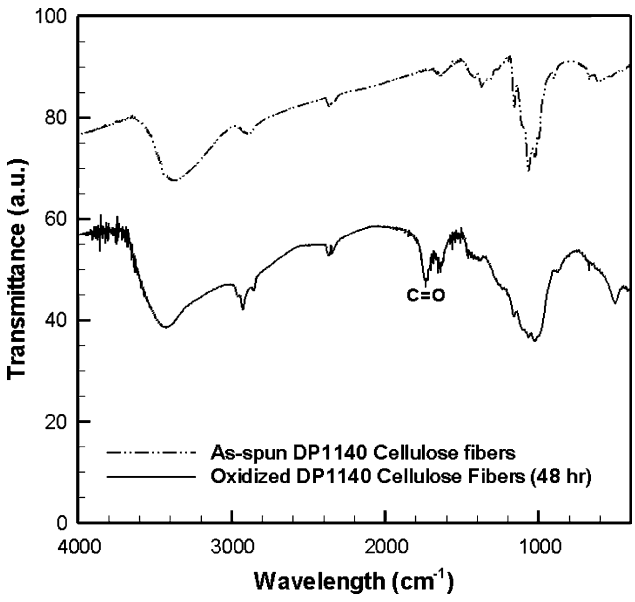

Fig. 12. FITR spectra of electrospun DP1140 cellulose fibers before and after 48 h of oxidation reaction.

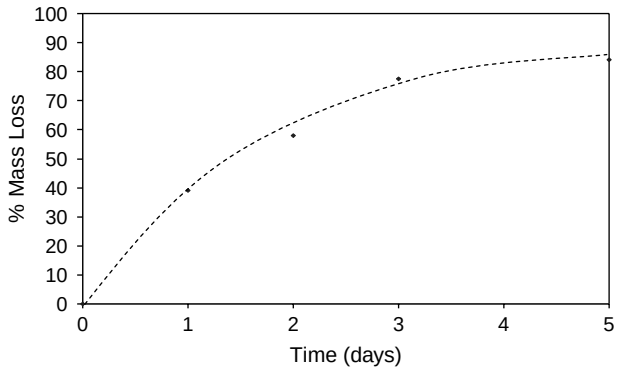

Fig. 13. Evolution of the degree of degradation profile of oxidized cellulose fibers in buffer solution with pH of 7 at 37 °C.

fibers reveal that applying coagulation with water right after the collection of fibers is necessary to obtain submicron scale, dry and stable cellulose fibers for both solution systems. X-ray diffraction studies reveal that cellulose fibers obtained from LiCl/DMAc are mostly amorphous, whereas the degree of crystallinity of cellulose fibers from NMMO/water can be controlled by various process conditions including spinning temperature, flow rate, and distance between the nozzle and collector.

Finally, electrospun cellulose fibers are oxidized by HNO_3/H_3PO_4 and $NaNO_2$, and the degradation characteristics of oxidized cellulose fibers under physiological conditions in an in vitro experiment have been presented. The degradation study of oxidized cellulose fibers suggests that the degradation time can be controlled possibly by controlling the average fiber diameter.

Acknowledgements

This work was supported in part by the NanoteK Consortium, Kraft Foods, Inc., and we would like to thank the Bill & Melinda Gates Foundation for funding, through a Gates Millennium Scholarship to C.W. Kim.

References

[1] Cuculo JA, Aminuddin N, Frey MW. In: Salem DR, editor. Structure formation in polymeric fiber. Munich: Hanser Gardner Publications, Inc.; 2001. p. 296–328 [chapter 8].
[2] Turbak AF, EL-Katrawy A, Synder FW, Auerbach AB. US Patent 4,302,252, Nov. 24; 1981.
[3] Liu H, Hsieh Y. J Polym Sci, Part B: Polym Phys 2002;40:2119–29.
[4] Fong H, Reneker DH. In: Salem DR, editor. Structure formation in polymeric fibers. Munich: Hanser Gardner Publications, Inc.; 2001. p. 225–46 [chapter 6].
[5] Shin YM, Hohman MM, Brenner MP, Rutledge GC. Appl Phys Lett 2001; 78:1149–51.
[6] Shin YM, Hohman MM, Brenner MP, Rutledge GC. Polymer 2001;42: 9955–67.
[7] Grafe TH, Graham KM. Proceeding of nonwovens in filtration—5th international conference. Stuttgart, Germany 2003.
[8] Graham K, Gogins M, Schreuder-Gibson H. Intl Nonwovens J 2004;13: 21–7.
[9] Mo XM, Xu CY, Kotaki M, Ramakrishna S. Biomaterials 2004;25: 1190–883.
[10] Min BM, Lee G, Kim SH, Nam YS, Park WH. Biomaterials 2004;25: 1289–97.
[11] Kang YS, Kim HY, Ryu YJ, Lee DR. J Korean Fiber Soc 2002;39:14–20.
[12] Kulpinski P. J Appl Polym Sci 2005;98:1855–9.
[13] Kim CW, Frey MW, Marquez M, Joo YL. J Polym Sci, Part B: Polym Phys 2005;43:1673–83.
[14] Röder T, Morgenstern B, Schelosky N, Glatter O. Polymer 2001;42: 6765–73.
[15] Matsumoto T, Tatsumi D, Tamai N, Takaki T. Cellulose 2001;8:275–82.
[16] El-Kafrawy A. J Appl Polym Sci 1982;27:2435–43.
[17] McCormick CL, Callais PA, Hutchinson BH. Macromolecules 1985;18: 2394–401.
[18] Biganska O, Navard P. Polymer 2003;44:1035–9.
[19] Kim DB, Lee WS, Jo SM, Lee YM, Kim BC. J Appl Polym Sci 2002;83: 981–9.
[20] Case F. Inform 2005;16:179.
[21] Kim D, Jo S, Lee W, Park J. J Appl Polym Sci 2004;93:1687–97.
[22] Rosenau T, Hofinger A, Potthast A, Kosma P. Polymer 2003;44:6153–8.
[23] Kumar V, Yang T. Carbohydr Polym 2002;48:403–12.
[24] Chae DW, Kim BC, Lee WS. J Appl Polym Sci 2002;86:216–22.
[25] Lewandowski Z. J Appl Polym Sci 2001;79:1860–8.
[26] Liu R, Shao H, Hu X. Macromol Mater Eng 2001;286:179–86.
[27] Rosenau T, Potthast A, Herbert S, Kosma P. Prog Polym Sci 2001;26: 1763–837.
[28] Isogai A. In: Gilbert RD, editor. Cellulosic polymers, blends and composites. Cincinnati, OH: Hanser Gardner Publications, Inc.; 1994. p. 1–21 [chapter 1].
[29] Zugenmaier P. Prog Polym Sci 2001;26:1341–417.
[30] Segal L, Creely JJ, Martin AE, Conrad CM. Textile Res J 1959;29: 786–94.
[31] Kasahara K, Sasaki H, Donkai N, Yoshihara T, Takagishi T. Cellulose 2001;8:23–8.
[32] Thygesen A, Oddershede J, Lilholt H, Thomsen AB, Stahl K. Cellulose 2005;15:563–76.
[33] Chanzy H, Dubé M, Marchessault RH. J Polym Sci, Polym Lett Ed 1979; 17:216–9.
[34] Biganska O, Navard P, Bédue O. Polymer 2002;43:6139–45.
[35] Kim DB, Lee YM, Lee WS, Jo SM, Kim BC. Euro Polym J 2002;83: 109–19.